

PAPER

# Capacity Estimation for Overlaid Multiband CDMA Systems with SIR-Based Power Control

Duk Kyung KIM<sup>†\*</sup>, *Nonmember* and Fumiyuki ADACHI<sup>†\*\*</sup>, *Regular Member*

**SUMMARY** As a flexible way to accommodate a variety of services, a number of spreading bands are now considered in International Mobile Telecommunications-2000 (IMT-2000) systems and more than two (overlaid) bands can be operated simultaneously in CDMA systems. Capacity estimation in CDMA systems is an important issue in performance analysis and call admission control (CAC), which is closely related to power control. This study derives the reverse link capacity of signal-to-interference ratio (SIR)-based power-controlled overlaid multiband CDMA systems in single and multiple cell environments. The weighted-aggregated data rate is introduced as the link capacity, which can reflect different spreading bandwidths and different QoS requirements. Various combinations of 5, 10, and 20 MHz subsystems are compared to one another in view of the maximum weighted-aggregated data rate. The impact of pulse shaping on CAC and the effect of multiple traffic accommodation on link capacity are also investigated.

**key words:** overlaid multiband CDMA systems, SIR-based power control, raised cosine filtered chip pulse

## 1. Introduction

Mobile communications services have deeply penetrated our society during the last two decades. Current second generation systems are successfully being operated in many countries, which are based on either time division multiple access (TDMA) or direct sequence code division multiple access (DS-SS) technologies. However, they are not expected to cope with the increasing demand for higher link capacity and for a variety of services including high-quality and high-rate services. Therefore, International Mobile Telecommunications-2000 (IMT-2000), as the third generation mobile communication system, is actively being developed for commercial services from 2001. Due to the numerous advantages over TDMA, such as soft handoff and the exploitation of multipath fading through Rake receivers, CDMA is a strong candidate for IMT-2000 systems. Since the current narrowband CDMA technology is not suitable for true IMT-2000 systems, a new technology called wideband CDMA is being developed throughout the world. In order to

flexibly accommodate various services, three spreading bands (5/10/20 MHz) are now considered for the IMT-2000 system [1]. When more than two bands are being operated simultaneously in a system, this system is called as a multiband system. In the initial phase of the commercial launch of IMT-2000 systems, a 5 MHz band may be implemented. Then, other bands will be added, keeping pace with the demand of mobile users and the development of technologies. One attractive feature of CDMA is the coexistence with other CDMA systems operating in the same frequency band [2], [3]. By virtue of this feature and due to the limited radio frequency band, using overlaid multiband systems is considered a flexible way to accommodate the services with a wide range of bit rates and quality-of-services (QoS).

Capacity estimation is an important issue in performance analysis and call admission control (CAC), which is closely related to power control schemes in CDMA systems. Many previous papers were based on strength-based power control. For example, Gilhousen et al. [4] calculated the capacity of systems supporting voice traffic and Ariyavisitakul [5] simulated a strength-based transmit power control (TPC) system. However, the signal-to-interference ratio (SIR)-based TPC is strongly recommended in IMT-2000 systems due to its potential for higher link performance [6]. This potential was probably, first indicated by Ariyavisitakul [7] using a simulation method in a constant bit rate (CBR) traffic environment. Lee and Sung [8], [9], and Kim and Sung [10] evaluated the capacity of DS-SS systems with an SIR-based TPC. However, they focused on a single cell environment. Kim and Sung [11] newly introduced a methodology for the reverse link capacity estimation for an SIR-based power-controlled system in a multiple cell environment and investigated the effects of the activity factor, the required signal energy per information bit-to-interference plus background noise spectrum density ratio  $E_b/I_o$ , the maximum received power, and propagation parameters on link capacity. Kim and Sung [12] also estimated the reverse link capacity for a multi-code CDMA system in terms of the admissible region in the CAC and investigated the effects of traffic and propagation parameters. All these studies, however, were based on systems with a single spreading band.

In overlaid multiband systems, Jeong et al. [13] an-

Manuscript received September 6, 1999.

Manuscript revised January 21, 2000.

<sup>†</sup>The authors are with the Wireless Laboratories, NTT DoCoMo, Inc., Yokosuka-shi, 239-8536 Japan.

\*Presently, with SK Telecom Central R&D Lab., Sungnam City, Kyunggi-do, Korea.

\*\*Presently, with the Department of Electrical Communications at Graduate School of Engineering, Tohoku University, Sendai-shi, 980-8579 Japan.

alyzed the reverse link capacity in a single cell environment in terms of the aggregated data rate. Adachi [14] also investigated the reverse link capacity for the case where users require different levels of QoS (or different required SIRs). However, they did not consider the spectral shaping by channel filtering of the spread signal and simply assumed that the signal power is uniformly distributed over an entire spreading band. Kim et al. [15], [16] considered the effect of channel filtering on the link capacity and proposed a radio resource management scheme in an overlaid multiband CDMA system. However, they considered a multiple cell system that simply included the other cell interference factor,  $f$ , where  $f$  is constant. As indicated in [11], [12], the value of  $f$  can be different according to the adopted power control scheme and the traffic environment. Moreover, for the capacity comparison of overlaid multiband CDMA systems, neither the aggregated data rate nor the number of users of each traffic type is suitable as performance measures. This is because the actual impact of users on link capacity depends on not only the data rate and the number of users, but also the required QoS as shown in [11], [12]. The weighted-aggregated data rate is newly introduced as the link capacity in this paper, which can reflect different spreading bandwidths and different QoS requirements.

This paper extends the studies of SIR-based TPC systems in [11], [12] to an overlaid multiband CDMA system. The reverse link capacity is estimated in single and multiple cell systems with multi-class CBR traffic. We assume a square root raised cosine Nyquist filter at both transmitter and receiver. Furthermore, the effect of a raised cosine filtered chip pulse on the mutual interference among the subsystems with different spreading bands is investigated. Various combinations of 5, 10, and 20 MHz subsystems are compared in terms of the maximum value of the weighted-aggregated data rate and some unique features are discussed in overlaid multiband CDMA systems.

Section 2 describes the system model and the assumptions. Section 3 reviews the relationship between the moment statistics of other cell interference and the received power in [11], [12], and the effect of a raised cosine filtered chip pulse on the mutual interference referring to [15], [16]. Section 4 derives the reverse link capacity of an overlaid multiband CDMA system with SIR-based TPC in a multiple cell environment. After showing numerical examples, Sect. 5 compares the capacities of various combinations and points out some unique features in an overlaid multiband CDMA system. Finally, Sect. 6 gives our conclusions.

## 2. System Model

To begin with, the following assumptions are used throughout the paper:

- 5/10/20 MHz spreading bandwidths are considered. Although there is no restriction on the spreading bandwidth and on the traffic type in the derivation of link capacity, three bandwidths are assumed for acquiring a good understanding and for numerical examples. Recently, these three bandwidths have been considered for the IMT-2000 system.
- A subsystem uses a single spreading bandwidth. Total allocated spreading bandwidth is assumed to be 20 MHz. Hence four 5 MHz, two 10 MHz, or one 20 MHz subsystem can be allocated in a system. There is no overlap between subsystems with the same spreading bandwidth and the center carrier frequency of each subsystem is located to maximize the number of available subsystems. Figure 1 shows all allocated subsystems together with the power spectral density (PSD) of the transmitted signal. Each subsystem is indexed from 1 to 7.
- Hexagonal cells of equal size are assumed and base stations (BSs) are located at the center of each cell. The subsystems with different spreading bandwidths share the same cell and the same BS receiver.
- The variable spreading factor method [1] is used for transmission of high rate traffic in a subsystem.

## 3. Preliminary

In [11], the relationship between the received power at a home BS and the Gaussian-modeled other cell interference from users who are power-controlled by other BSs was derived for a single type of traffic. Section 3.1 reviews this relationship.

In general the chip waveform is an important factor in determining the link performance. Moreover, in an overlaid multiband CDMA system, the shape of PSD, which depends on the chip waveform, determines the mutual interference among the subsystems with different spreading bands. The rectangular chip waveform was previously used in [11], [12], but the raised cosine filtered chip pulse with a roll-off factor of  $\alpha$  will be adopted for IMT-2000 systems (i.e., a square root raised cosine Nyquist filter is used for transmitter and receiver filters) in order to reduce both the intersymbol effect and the spectral width of the modulated signal [20]. Section 3.2 reviews the effect of the raised cosine filtered chip pulse referring to [15], [16].

### 3.1 Relationship between Received Power and Other Cell Interference

The relationship between the received signal power,  $S$ , and the other cell interference power,  $I_{other}$ , was derived in a non-fading environment in [11], [12]. The

following were assumed:

- Ideal hexagonal cell structure with a unit cell radius.
- The zero-th cell and 18 other cells indexed  $m$  in the first and second tiers.
- Spatially uniform density of users  $\rho = \frac{2N}{3\sqrt{3}}$ , where  $N$  is the number of users of each cell.
- Perfect power control.
- The best cell site that has the least product of path loss and shadowing is always selected for communication (this is equivalent to selection-type soft handoff).
- Gaussian model for other cell interference.

Let  $\mu$  be the path loss exponent and the shadowing follow a log normal process with standard deviation  $\sigma$  dB and mean = 0 dB. Then, the mean,  $m_I$ , and the variance,  $\sigma_I^2$ , of other cell interference power can be approximated as [11], [12]

$$m_I \approx M(\mu, \sigma)E[S]N, \quad (1)$$

$$\sigma_I^2 \approx \{A(\mu, \sigma)E[S^2] - B(\mu, \sigma)E^2[S]\}N, \quad (2)$$

where  $E[\cdot]$  is an ensemble operation and  $M(\mu, \sigma)$ ,  $A(\mu, \sigma)$ , and  $B(\mu, \sigma)$  are given by:

$$M(\mu, \sigma) = e^{\{\sigma \ln(10)/10\}^2} \iint \left(\frac{r_m}{r_0}\right)^\mu \cdot \Phi \left( \frac{10\mu}{\sqrt{2\sigma^2}} \log_{10}(r_o/r_m) - \sqrt{2\sigma^2} \frac{\ln(10)}{10} \right) \rho' dA,$$

$$A(\mu, \sigma) = e^{\{\sigma \ln(10)/5\}^2} \iint \left(\frac{r_m}{r_0}\right)^{2\mu} \cdot \Phi \left( \frac{10\mu}{\sqrt{2\sigma^2}} \log_{10}(r_o/r_m) - \sqrt{2\sigma^2} \frac{\ln(10)}{5} \right) \rho' dA,$$

$$B(\mu, \sigma) = e^{2\{\sigma \ln(10)/10\}^2} \iint \left(\frac{r_m}{r_0}\right)^{2\mu} \cdot \Phi^2 \left( \frac{10\mu}{\sqrt{2\sigma^2}} \log_{10}(r_o/r_m) - \sqrt{2\sigma^2} \frac{\ln(10)}{10} \right) \rho' dA,$$

respectively, and  $r_m$  is the distance from an mobile station (MS) to the  $m$ -th BS, and  $\rho'$  and  $\Phi(x)$  are expressed as

$$\rho' = \rho/N,$$

$$\Phi(x) = \frac{1}{\sqrt{2\pi}} \int_{-\infty}^x e^{-y^2/2} dy.$$

The values of  $M(\mu, \sigma)$ ,  $A(\mu, \sigma)$ , and  $B(\mu, \sigma)$  are denoted as  $M$ ,  $A$ , and  $B$ , respectively.  $M$ ,  $A$ , and  $B$  depend only on  $\mu$  and  $\sigma$ , and are independent of the traffic type.  $M$ ,  $A$ , and  $B$  can be numerically obtained by considering the first and second tiers. For  $\mu = 4$  and  $\sigma = 8$  dB,  $M = 0.659$ ,  $A = 0.223$ , and  $B = 0.04$ .

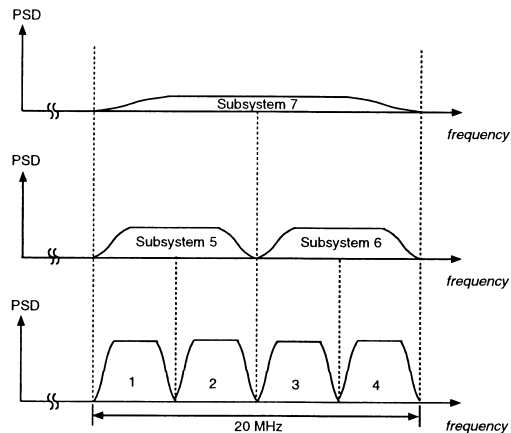


Fig. 1 PSD  $h(f)$  of the transmitted signal.

### 3.2 Effect of Raised Cosine Pulse Shaping

The raised cosine spectrum is widely used in practice and its composite transfer function,  $H(f)$ , of transmitter and receiver filters with a roll-off factor of  $\alpha$  ( $0 \leq \alpha \leq 1$ ) is given by [19], [20]

$$H(f) = \begin{cases} 1, & \text{for } 0 \leq |f - f_c| < \frac{1 - \alpha}{2T_c}, \\ \frac{1}{2} \left[ 1 - \sin \left( \frac{2\pi|f - f_c|T_c - \pi}{2\alpha} \right) \right], & \text{for } \frac{1 - \alpha}{2T_c} \leq |f - f_c| \leq \frac{1 + \alpha}{2T_c}, \\ 0, & \text{otherwise,} \end{cases} \quad (3)$$

where  $T_c$  denotes the chip duration and  $f_c$  is the center carrier frequency. The RF passband bandwidth  $B$  is given as [20]

$$B = \frac{1}{T_c}(1 + \alpha).$$

In this paper the value of  $1/T_c$  is set to 4.096 Mcps, 8.192 Mcps, and 16.384 Mcps for 5 MHz, 10 MHz, and 20 MHz spreading bandwidths, respectively, when  $\alpha$  is set to 0.22. The PSD  $h(f)$  of the received signal can be expressed as

$$h(f) = \frac{SH(f)}{\int_{-\infty}^{\infty} H(f)df},$$

where  $S$  is the received signal power. In Fig. 1,  $h(f)$  is obtained assuming that  $S$  is the same for all subsystems to see the effect of pulse shaping.

In an overlaid multiband CDMA system, the mutual interferences among different subsystems can be determined by the PSD of the transmitted signal and the transfer function of the receive filter. Let  $S_k$  be the power of a user received at a BS in subsystem  $k$ . The interference suppression factor,  $\xi_{km}$ , from subsystem  $k$

to subsystem  $m$  was newly introduced in [16], which is defined as

$$\xi_{km} \triangleq \frac{S_{km}}{S_k}, \quad (4)$$

where  $S_{km}$  ( $0 \leq S_{km} \leq S_k$ ) is the power portion of  $S_k$  received by the BS receiver in subsystem  $m$ . (4) can be simply expressed as [21]

$$\xi_{km} = \frac{\int H_k(f)H_m(f)df}{\int H_k(f)df}, \quad (5)$$

where  $H_k(f)$  is  $H(f)$  in subsystem  $k$ . More precisely, the interference power of another user in subsystem  $k$  is suppressed by a factor of  $\xi_{km}$  at a desired user's receiver in subsystem  $m$  through the chip waveform matched filter. Interference power from other users are further suppressed, divided by the spreading factor through the code matched filter (or correlator) for a random spreading code. We assumed asynchronous CDMA systems, where the interference user is asynchronous to the desired user (this is true in the reverse link). When  $k = m$ ,  $\xi_{km}$  is readily expressed as

$$\xi_{mm} = 1 - \frac{\alpha}{4},$$

which is 0.945 for  $\alpha = 0.22$  [22]. On the other hand, for the case of rectangular chip pulse, it is  $2/3$ .

#### 4. Reverse Link Capacity

CBR traffic with different data rates and different QoS requirements are considered. Let  $K$  denote the number of subsystems and  $T$  denote the number of traffic types. A user of traffic type  $t$  is called a type- $t$  user and is assumed to have a data rate of  $R_t$ . A type- $t$  user requires an  $E_b/I_o$  target value of  $\gamma_{t(m)}$  in subsystem  $m$ . Even though the same type- $t$  users require the same bit error rate (BER), the value of  $\gamma_{t(m)}$  may differ according to the spreading bandwidth and the adopted channel coding scheme. Let us consider that a total  $n_{t(m)}$  of type- $t$  users are in communication in subsystem  $m$  and their received signal power levels at their home BSs are denoted as  $S_{t(m)}$ . In an SIR-based TPC system,  $S_{t(m)}$  is a random variable according to the interference level. If  $W_{(m)}$  is the chip rate of subsystem  $m$ ,  $G_{t(m)} (\triangleq W_{(m)}/R_t)$  is processing gain  $G$  of a type- $t$  user in subsystem  $m$ .

##### 4.1 $E_b/I_o$ Equation

Referring to [8], [16], the  $E_b/I_o$  of a type- $t$  user in system  $m$  can be expressed as

$$\left(\frac{E_b}{I_o}\right)_{t(m)} \triangleq \frac{G_{t(m)}S_{t(m)}}{\left\{ \sum_{k=1}^K \xi_{km} \left( \sum_{i=1}^T n_{i(k)} S_{i(k)} \right) - S_{t(m)} + I_{(m)} + 1 \right\}}, \quad (6)$$

where  $I_{(m)}$  is the other cell interference power in subsystem  $m$ . It is noted that all types of users in the same subsystem endure the same amount of other cell interference. It is also noted that, in (6), the signal power and interference power are normalized by background noise power  $\eta_o W_{(m)}$  in the subsystem of interest, where  $\eta_o/2$  is the two-sided background noise power spectrum density (thus, now  $S_{t(m)}$  and  $I_{(m)}$  denote the signal-to-noise power ratio (SNR) and the interference-to-noise power ratio (INR), respectively). The definition in (6) is based on a Gaussian density approximation used to evaluate the BER in an asynchronous DS-CDMA system when an additive white Gaussian noise (AWGN) process and random signature sequences are assumed [18].

Assuming all users are power controlled to maintain minimum power levels satisfying  $(E_b/I_o)_{t(m)} = \gamma_{t(m)}$ , (6) can be rewritten as

$$\begin{aligned} \sum_{k=1}^K \xi_{km} \left( \sum_{i=1}^T n_{i(k)} S_{i(k)} \right) + I_{(m)} + 1 \\ = S_{t(m)} \left( \xi_{mm} + \frac{G_{t(m)}}{\gamma_{t(m)}} \right), \text{ for all } m, t. \end{aligned} \quad (7)$$

Readily, from (7), the received powers of type- $t$  users in subsystem  $m$  satisfy the following relationships

$$S_{t(m)} = \frac{\left( \xi_{mm} + \frac{G_{1(m)}}{\gamma_{1(m)}} \right)}{\left( \xi_{mm} + \frac{G_{t(m)}}{\gamma_{t(m)}} \right)} S_{1(m)}. \quad (8)$$

The above equation can be simplified as

$$S_{t(m)} = \beta_{t(m)} S_{1(m)}, \quad (9)$$

where

$$\beta_{t(m)} \triangleq \frac{\left( \xi_{mm} + \frac{G_{1(m)}}{\gamma_{1(m)}} \right)}{\left( \xi_{mm} + \frac{G_{t(m)}}{\gamma_{t(m)}} \right)}.$$

Substitution of (9) into (7) yields

$$\begin{aligned} \sum_{k=1}^K \xi_{km} \left( \sum_{t=1}^T n_{t(k)} \beta_{t(k)} S_{1(k)} \right) + I_{(m)} + 1 \\ = S_{1(m)} \left( \xi_{mm} + \frac{G_{1(m)}}{\gamma_{1(m)}} \right), \text{ for all } m. \end{aligned} \quad (10)$$

If we use the following definitions:

$$\begin{aligned} S_{(k)} &\triangleq S_{1(k)}, \\ G_{(m)} &\triangleq G_{1(m)}, \\ \gamma_{(m)} &\triangleq \gamma_{1(m)}, \\ \tilde{n}_{(k)} &\triangleq \sum_{t=1}^T n_{t(k)} \beta_{t(k)}, \end{aligned}$$

(10) reduces to

$$\begin{aligned} & \sum_{k=1}^K \xi_{km} \tilde{n}_{(k)} S_{(k)} + I_{(m)} + 1 \\ & = S_{(m)} \left( \xi_{mm} + \frac{G_{(m)}}{\gamma_{(m)}} \right). \end{aligned} \quad (11)$$

A Gaussian model is adopted for other cell interference power  $I_{(m)}$  in subsystem  $m$ . If received powers of differently-located MSs are assumed to be mutually independent regardless of traffic type, it was indicated in [12] that  $I_{(m)}$  can be obtained as the sum of the independent Gaussian-modeled other cell interference power of each traffic type. In an overlaid multiband CDMA system, the power level of  $\xi_{km} S_{t(k)}$  is received at the BS receiver of subsystem  $m$  from a type- $t$  user in subsystem  $k$ , and  $\xi_{km}$  is independent of the traffic type. Hence from (1) and (2), mean  $m_{I_{(m)}}$  and variance  $\sigma_{I_{(m)}}^2$  of  $I_{(m)}$  can be expressed as [4], [11], [12]:

$$m_{I_{(m)}} = \sum_{k=1}^K \xi_{km} M \sum_{t=1}^T n_{t(k)} E[S_{t(k)}], \quad (12)$$

$$\begin{aligned} \sigma_{I_{(m)}}^2 & = \sum_{k=1}^K \xi_{km}^2 \left( A \sum_{t=1}^T n_{t(k)} E[S_{t(k)}^2] \right. \\ & \quad \left. - B \sum_{t=1}^T n_{t(k)} E^2[S_{t(k)}] \right). \end{aligned} \quad (13)$$

From (9), (12) and (13) reduce to

$$m_{I_{(m)}} = \sum_{k=1}^K \xi_{km} M \tilde{n}_{(k)} E[S_{(k)}], \quad (14)$$

$$\begin{aligned} \sigma_{I_{(m)}}^2 & = \sum_{k=1}^K \xi_{km}^2 \left( A \sum_{t=1}^T n_{t(k)} \beta_{t(k)}^2 E[S_{(k)}^2] \right. \\ & \quad \left. - B \sum_{t=1}^T n_{t(k)} \beta_{t(k)}^2 E^2[S_{(k)}] \right). \end{aligned} \quad (15)$$

To compute the BER based on Gaussian approximation, we need to know  $m_{I_{(m)}}$  and  $\sigma_{I_{(m)}}^2$ .

#### 4.2 Obtaining $m_{I_{(m)}}$ and $\sigma_{I_{(m)}}^2$

By taking the expectation of both sides of (11) and by substituting (14) into (11), the following relations are obtained

$$\begin{aligned} & \sum_{k=1}^K \xi_{km} \tilde{n}_{(k)} E[S_{(k)}] (1 + M) + 1 \\ & = \left( \xi_{mm} + \frac{G_{(m)}}{\gamma_{(m)}} \right) E[S_{(m)}], \text{ for all } m. \end{aligned} \quad (16)$$

From (16),  $E[S_{(m)}]$  is obtained (this is also used later

to obtain  $\sigma_{I_{(m)}}^2$ ). Using (14),  $m_{I_{(m)}}$  can be obtained.

To obtain  $\sigma_{I_{(m)}}^2$ , we first express (11) as

$$\mathbf{A}\mathbf{S} = \mathbf{B}, \quad (17)$$

where

$$\mathbf{S} = \begin{bmatrix} S_{(1)} \\ \vdots \\ S_{(K)} \end{bmatrix},$$

$\mathbf{A}$  is a  $K \times K$  matrix, and  $\mathbf{B}$  is a  $K \times 1$  column vector. Elements  $a_{mh}$  of  $\mathbf{A}$  can be given by

$$a_{mh} = \begin{cases} \xi_{mm} + \frac{G_{(m)}}{\gamma_{(m)}} - \xi_{mm} \tilde{n}_{(m)}, & \text{if } m = h \\ -\xi_{hm} \tilde{n}_{(h)}, & \text{otherwise,} \end{cases} \quad (18)$$

and elements  $b_m$  of  $\mathbf{B}$  can be expressed as

$$b_m = I_{(m)} + 1. \quad (19)$$

From (17),  $\mathbf{S}$  can be obtained by

$$\mathbf{S} = \mathbf{A}^{-1} \mathbf{B} \triangleq \mathbf{C}\mathbf{B}. \quad (20)$$

Therefore,  $S_{(m)}$  can be expressed as the weighted sum of INR in each subsystem. If the other cell interference in each subsystem is assumed to be mutually independent of one another, the variance of  $S_{(m)}$  can be obtained as the sum of variances  $\sigma_{I_{(k)}}^2$ . Hence  $E[S_{(m)}^2]$  can be easily obtained from (20):

$$E[S_{(m)}^2] = \sum_{k=1}^K c_{mk}^2 \sigma_{I_{(k)}}^2 + E^2[S_{(m)}], \quad (21)$$

where  $c_{mk}$  is an element in the  $m$ -th row and  $k$ -th column of  $\mathbf{C}$ .

The steps for calculation are as follows:

1. Calculate  $E[S_{(m)}]$  and  $m_{I_{(m)}}$  for all  $m$  from (14) and (16).
2. Set all  $\sigma_{I_{(m)}}^2$  to zero.
3. Calculate  $E[S_{(m)}^2]$  from (21).
4. Calculate  $\sigma_{I_{(m)}}^2$  from (15).
5. Repeat steps 3 and 4 until the errors of  $\sigma_{I_{(m)}}^2$  are within a given bound. For numerical examples, the sum of errors is set to be less than 1%.

#### 4.3 Computing Capacity

When all MSs satisfy the required  $E_b/I_o$ , this is called the normal state. Then, the link enters an outage state if one or more than one MS can no longer satisfy the required  $E_b/I_o$ , i.e., if the required signal power level is

greater than the maximum allowable value. In mathematical analysis, when too many users are accommodated in a system, the required signal power level can be calculated as a negative value in (20), which is also considered here as an outage state. From the mean and variance statistics in (16) and (21), the outage probability can be obtained for each subsystem. If  $P_{(m),out}$  is the outage probability of subsystem  $m$  and  $\mathbf{N}$  is the matrix of  $n_{t(m)}$  ( $1 \leq m \leq K$ ,  $1 \leq t \leq T$ ), the admissible region can be expressed as  $\mathbf{N}$  satisfying

$$P_{(m),out} \leq o_m, \quad (22)$$

where  $o_m$  is the maximum allowable outage probability of subsystem  $m$ . To obtain a tolerable BER for all subsystems,  $\mathbf{N}$  should satisfy (22) for all  $m$ .

Weighted-aggregated data rate  $R_{wa}$  is newly introduced as the link capacity:

$$R_{wa} \triangleq R_1 \sum_{k=1}^K \tilde{n}_{(k)} = R_1 \sum_{k=1}^K \sum_{t=1}^T n_{t(k)} \beta_{t(k)}, \quad (23)$$

where  $\beta_{t(k)}$  is a weighting factor that depends on the processing gain and the required  $E_b/I_o$  of a type- $t$  user in subsystem  $k$ . Factor  $\beta_{t(k)}$  is defined as the ratio of the received powers of type- $t$  and type-1 users (see (9)). Thus, the type- $t$  user produces  $\beta_{t(k)}$  times larger interference power than the type-1 user. From this,  $n_{t(k)} \beta_{t(k)}$  denotes the equivalent number of type-1 users for a type- $t$  user in subsystem  $k$ . Hence  $R_{wa}/R_1$  physically represents the equivalent number of type-1 users accommodated in a system.

As a special case, let us consider a single cell system. There is no other cell interference in a single cell system. By setting

$$I_{(m)} = 0, \text{ for all } m$$

in (19), we can obtain the required SNR level,  $S_{(m)}$ , of each system from (17). Then, we can determine the admissible region satisfying the following condition:

$$\{S_{(m)} : 0 \leq S_{(m)} \leq S_{(m),max} \text{ for all } m\}, \quad (24)$$

where  $S_{(m),max}$  is the maximum received SNR of a type-1 user in subsystem  $m$ .

## 5. Numerical Examples

In the following numerical computations, we use  $T = 3$  and  $K = 7$  as indicated in Table 1 and Fig. 1. Table 1 shows three representative traffic types: voice (8 kbps), fax (64 kbps), and video (128 kbps). Each traffic transmits its data at a constant rate. Four combinations are considered as the numerical examples.

- Case A: Subsystems 1, 2, 3, and 4 are initially implemented.

**Table 1** Traffic parameters.

	Index ( $t$ )	Data rate ( $R_t$ )	$E_b/I_o$ target
Low-rate (voice)	1	8 kbps	3.34 dB
Medium-rate (fax)	2	64 kbps	2.3 dB
High-rate (video)	3	128 kbps	1.6 dB

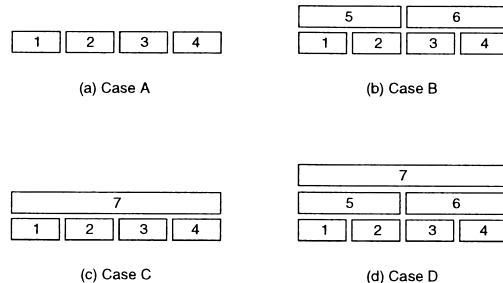


**Fig. 2** Conceptual description of four cases.

**Table 2** System parameters.

$S_{(1),max}$ (voice)	0 dB
$\alpha$ (roll-off factor)	0.22
$\mu$	4
$\sigma$	8 dB

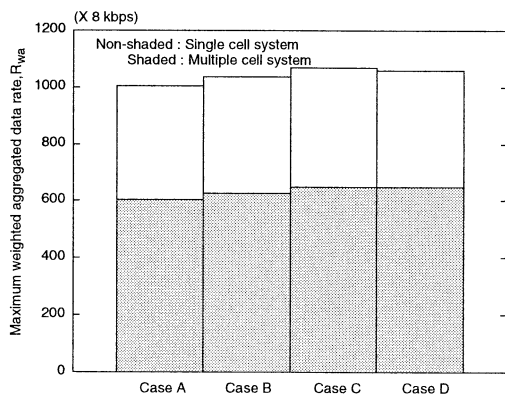
- Case B: Subsystems 5 and 6 are additionally added to case A.
- Case C: Subsystem 7 is supplemented to case A.
- Case D: All seven subsystems are operated together.

Figure 2 conceptually describes these four cases. Unless otherwise stated, for computational simplicity, only fax traffic is assumed to be accommodated in subsystems 5 and 6, and only video traffic is assumed to be accommodated in subsystem 7 in a multiple cell environment. However, the impact of multiple traffic accommodation will be discussed later in this section.

The required  $E_b/I_o$  strongly depends on the required BER and the adopted performance-enhancing technology. The different values of  $E_b/I_o$  are determined based on the computer simulation results in [17] and in our computer simulation. In the following, voice traffic is assumed to require an  $E_b/I_o$  of 3.34 dB to achieve the BER of  $10^{-3}$  when a convolutional code of rate 1/3 and an interleaving length of 10 msec are adopted. For fax and video, an interleaving length of 80 msec and a turbo code of rate 1/3 are used in a Rayleigh fading environment with the Vehicular-B power delay profile [17]. These two traffic types require  $E_b/I_o$  values of 2.3 dB and 1.6 dB, respectively, to achieve the BER of  $10^{-6}$  (the effect of a different target value of  $E_b/I_o$  is described in [11], [12]). Table 2 shows the system parameters, where roll-off factor  $\alpha$  of a raised cosine filter is set to 0.22.  $S_{(1),max} = 0$  dB corresponds to the signal energy per information bit-to-background noise density ratio of a type-1 (voice)

**Table 3** The values of interference suppression factors  $\xi_{km}$ .

$k \setminus m$	1	2	3	4	5	6	7
1	0.945	0	0	0	0.881	0	0.667
2	0	0.945	0	0	0.881	0	1
3	0	0	0.945	0	0	0.881	1
4	0	0	0	0.945	0	0.881	0.667
5	0.441	0.441	0	0	0.945	0	0.881
6	0	0	0.441	0.441	0	0.945	0.881
7	0.167	0.250	0.250	0.167	0.441	0.441	0.945

**Fig. 3** Comparison of the maximum value of weighted-aggregated data rate  $R_{wa}$  within the admissible region.

user,  $(E_b/\eta_o)_{(1),max} = G_{(1)}S_{(1),max} = 27.1$  dB. Only the maximum received SNR of voice traffic is shown in Table 2. The maximum received SNRs of the other traffic types are assumed to keep the relations:

$$S_{1(m),max} = \frac{S_{2(m),max}}{\beta_{2(m)}} = \frac{S_{3(m),max}}{\beta_{3(m)}}. \quad (25)$$

The values of interference suppression factor  $\xi_{km}$  are listed in Table 3. It is noted that the effect of subsystem 7 on subsystem 1 is smaller than the effect on subsystem 2 or 3 because the signal power is mainly concentrated at the center of the band.

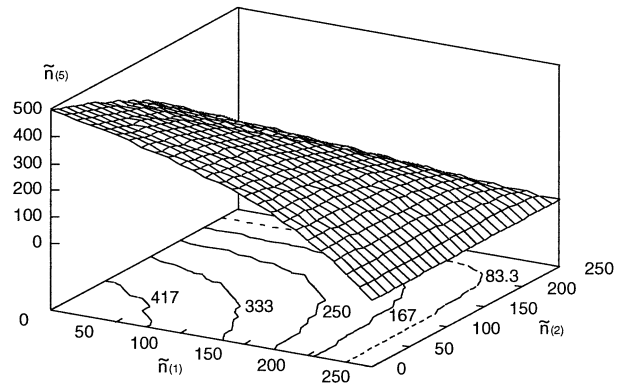
In (22), the values of  $o_m$  are set to 0.01 for all  $m$  and  $P_{out}$  denotes the maximum value of  $P_{(m),out}$  ( $1 \leq m \leq K$ ). Then, the admissible region should satisfy the following condition:

$$P_{out} \leq 0.01.$$

This condition is used throughout the paper (the effect of different maximum allowable outage probability can be found in [12]).

### 5.1 Comparison of the Maximum Capacity

Figure 3 shows comparisons of the maximum value of  $R_{wa}$  within the admissible region in single and multiple cell systems for four cases. When two subsystems with a 10 MHz spreading bandwidth are implemented instead of four subsystems with a 5 MHz spreading bandwidth (i.e., subsystems 5 and 6 instead of subsystems 1, 2, 3, and 4), the link capacity is approximately

**Fig. 4** Admissible region boundary for a single cell system when only subsystems 1, 2, and 5 are considered in Case B.

the same because the required  $E_b/I_o$  of a type- $t$  user is assumed to be constant regardless of the spreading bandwidth and the capacity is limited by mutual interference rather than by background noise (the effect of the maximum received power is described in [11]). Similarly, if only subsystem 7 is used, the link capacity is approximately the same as the capacity of subsystems 1, 2, 3, and 4. It is interesting to note from Fig. 3 that it does not degrade the capacity, but yields a slight capacity gain to supplement subsystems 5, 6, and 7. Cases B and C yield approximately 3.2% and 6.6% capacity gains compared to Case A. There is still inefficient bandwidth usage around the boundaries of the spread band, even though a raised cosine filtered chip pulse is used to mitigate this problem. This inefficiency can be reduced by overlapping subsystems with different spreading bandwidths. However, supplementing Case C with subsystems 5 and 6 (i.e., Case D) does not provide any capacity gain because the mutual interference among subsystems offsets the capacity gain. The multiple cell capacity is approximately 60% of the single cell capacity, which was indicated in [11] in a CBR traffic environment.

### 5.2 Case B

In Case B, subsystems 1, 2, and 5 are mutually independent of subsystems 3, 4, and 6. Figure 4 shows the admissible region boundary for a single cell system when only subsystems 1, 2, and 5 are considered in Case B. Notations  $\tilde{n}_{(1)}$ ,  $\tilde{n}_{(2)}$ , and  $\tilde{n}_{(5)}$  are used instead of  $n_1$ ,  $n_2$ , and  $n_5$  ( $\tilde{n}_{(m)}$  denotes the equivalent number of type-1 users in subsystem  $m$ ). In a single cell system, the link capacity is affected only by  $\tilde{n}_{(m)}$ ,  $m = 1, 2, \text{ and } 5$ , which can be expected from (11). Thus, the single cell capacity does not depend on whether or not multiple types of traffic are accommodated in a subsystem. In a multiple cell system, the number of users of each traffic type affects the variance statistics as shown in (15). If more users are accommodated in subsystem  $m$  for the same value of  $\tilde{n}_{(m)}$ , a reduction in variance

can be expected. The effect of multiple traffic accommodation will be discussed later.

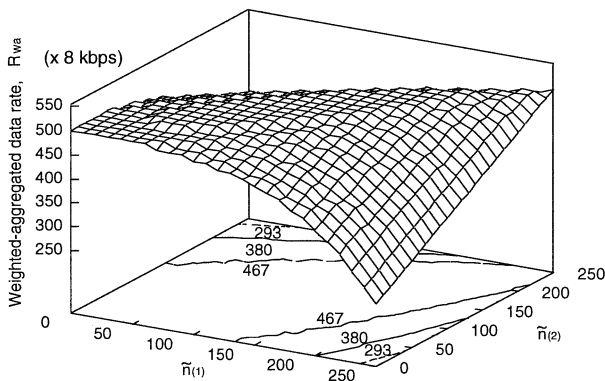
Figure 5 shows the value of  $R_{wa}$  at the admissible region boundaries in Fig. 4. Note that  $R_{wa}$  is not constant at the boundaries. The achievable capacity differs from point to point. This means there is a need for a special CAC to maximize the link capacity. In Case B, the capacity is symmetrical on the axis of  $\tilde{n}_{(2)} = \tilde{n}_{(1)}$ . CAC problems will be discussed in more detail in Sect. 5.3.

Figure 6 shows the admissible region boundary for a multiple cell system in the same situation as in Fig. 4. The width of a staircase varies according to the set of  $\tilde{n}_{(1)}$ ,  $\tilde{n}_{(2)}$ , and  $\tilde{n}_{(5)}$ . In an SIR-based TPC system, the power level varies according to the received interference

level. Furthermore, this power level determines its impact on link capacity. Table 4 shows the average values of  $S_{(1)}$ ,  $S_{(2)}$ , and  $\beta_{2(5)}S_{(5)}$  for different sets of  $\tilde{n}_{(1)}$ ,  $\tilde{n}_{(2)}$ , and  $\tilde{n}_{(5)}$ . The ratio of  $\beta_{2(5)}E[S_{(5)}]$  over  $E[S_{(1)}]$  determines the relative impact on link capacity of fax users in subsystem 5 compared with voice users in subsystem 1. As the ratio increases, the width of the staircase becomes wider.

### 5.3 Relation to CAC

Figures 7(a) and (b) show the probability density functions (pdfs) of  $R_{wa}$  at admissible region boundaries in Cases B and C, respectively. In Case B, only subsystems 1, 2, and 5 are considered. The link capacity varies in a wide range at the admissible region boundaries. As mentioned before, this wide variation necessitates a



**Fig. 5** Weighted-aggregated data rate  $R_{wa}$  at admissible region boundaries for a single cell system when only subsystems 1, 2, and 5 are considered in Case B.

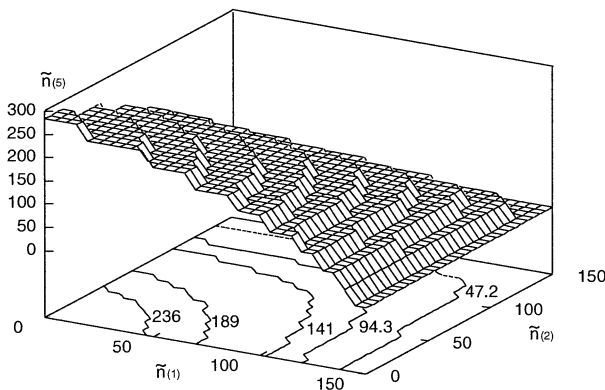
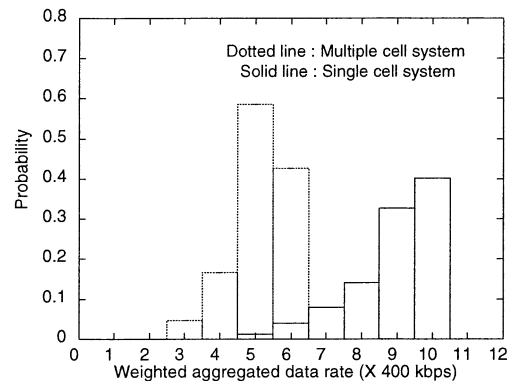
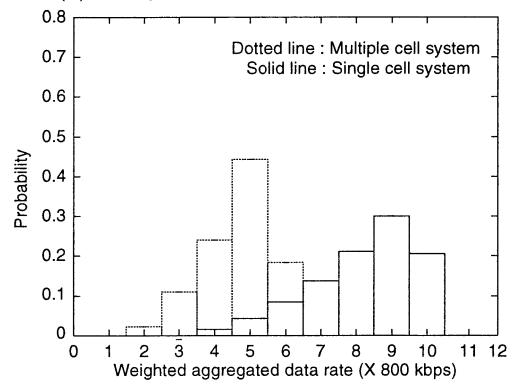


**Fig. 6** Admissible region boundary for a multiple cell system when only subsystems 1, 2, and 5 are considered in Case B.



(a) Subsystems 1, 2, and 5 in Case B.



(b) Case C.

**Fig. 7** The probability density functions (pdfs) of weighted-aggregated data rate  $R_{wa}$  at admissible region boundaries.

**Table 4** The values of  $E[S_{(1)}]$ ,  $E[S_{(2)}]$ , and  $\beta_{2(5)}E[S_{(5)}]$  for different sets of  $\tilde{n}_{(1)}$ ,  $\tilde{n}_{(2)}$ , and  $\tilde{n}_{(5)}$  in a multiple cell system in case B (Unit: dB).

$\tilde{n}_{(1)}$	$\tilde{n}_{(2)}$	$\tilde{n}_{(5)}$	$E[S_{(1)}]$	$E[S_{(2)}]$	$\beta_{2(5)}E[S_{(5)}]$	$\frac{\beta_{2(5)}E[S_{(5)}]}{E[S_{(1)}]}$	$\frac{\beta_{2(5)}E[S_{(5)}]}{E[S_{(2)}]}$
90	10	125	-15.74	-19.35	-12.19	6.55	10.16
20	10	251	-13.73	-14.05	-8.67	8.06	8.38
20	20	251	-11.98	-11.98	-8.77	8.21	8.21
90	90	125	-8.46	-8.46	-3.52	7.94	7.94



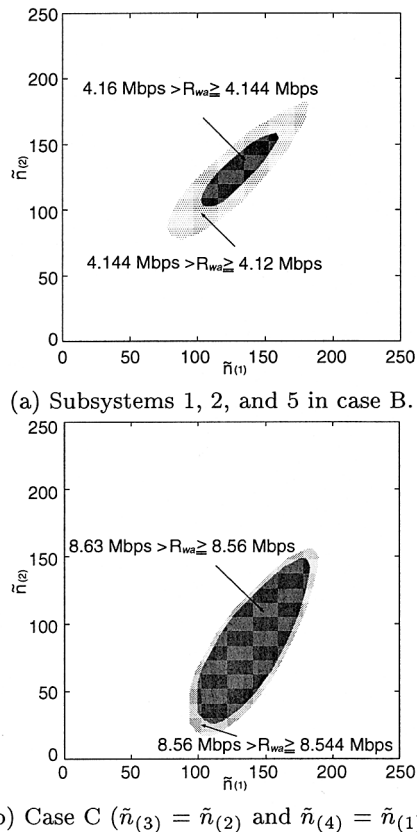


**Fig. 8** Admissible regions satisfying weighted-aggregated data rate  $R_{wa} \geq$  a given value in a single cell environment.

special CAC scheme to maximize the link capacity.

Investigating which points maximize the link capacity is closely related to how to perform CAC. Figure 8(a) shows the admissible points where the link capacity is larger than or equal to 4.144 Mbps and 4.12 Mbps in case B having only subsystems 1, 2, and 5. The link capacity is maximized at the points where subsystems 1 and 2 are equally loaded because  $\xi_{15} = \xi_{25}$  and  $\xi_{51} = \xi_{52}$ . The traffic ratio  $(\tilde{n}_{(1)} + \tilde{n}_{(2)})/\tilde{n}_{(5)}$  is approximately determined as  $\frac{2(\xi_{51} + \xi_{52})}{\xi_{15} + \xi_{25}}$  ( $=1$ ), where the factor of 2 represents the effect of the different processing gains. Figure 8(b) shows the admissible points that make the link capacity larger than or equal to 8.544 Mbps and 8.56 Mbps in case C with  $\tilde{n}_{(4)} = \tilde{n}_{(1)}$  and  $\tilde{n}_{(3)} = \tilde{n}_{(2)}$ . The different influences between subsystems 7 and 1, and between subsystems 7 and 2 differ from the trend in Case B. The maximum capacity can be achieved around the points where  $\frac{\tilde{n}_{(1)}}{\tilde{n}_{(2)}} \approx \frac{\xi_{72}}{\xi_{71}}$  ( $=1.5$ ). Similarly, the relation between  $\tilde{n}_{(7)}$  and  $\tilde{n}_{(1)} + \tilde{n}_{(2)} + \tilde{n}_{(3)} + \tilde{n}_{(4)}$  can be obtained by the interference suppression factors,  $\xi_{km}$ , among the subsystems. In summary, the interference suppression factors can be used to determine how to perform CAC in overlaid multiband CDMA systems.

A precise CAC as mentioned above is rather complicated in a real system. Let us consider a simple CAC,

**Table 5** Mean  $m_{I_{(7)}}$  and variance  $\sigma_{I_{(7)}}^2$  of  $I_{(7)}$  in a multiple cell system in case C for  $\tilde{n}_{(1)} = \tilde{n}_{(2)} = \tilde{n}_{(3)} = \tilde{n}_{(4)} = 10$  (No:  $n_{1(7)} = n_{2(7)} = 0$ , Yes:  $n_{1(7)} = n_{2(7)} = n_{3(7)}$ , and Unit: dB).

	$m_{I_{(7)}}$		$\sigma_{I_{(7)}}^2$	
	No	Yes	No	Yes
$\tilde{n}_{(7)} = 54$	-6.20	-6.18	-28.10	-28.91
$\tilde{n}_{(7)} = 397$	5.52	5.50	-10.08	-10.99

where traffic load normalized by the spreading bandwidth is equally distributed in each subsystem. We found from another numerical computation that when a simple CAC is adopted for a single cell system in Case C, the maximum link capacity is 8.28 Mbps for the raised cosine filtered chip pulse with  $\alpha = 0.22$ . Compared to the maximum link capacity obtained by precise CAC, capacity degradation is approximately 4.1% (degradation of 350 kbps from 8.63 Mbps) if the raised cosine filtered chip pulse is used with  $\alpha = 0.22$ .

#### 5.4 Multiple Traffic Accommodation

To investigate the effect of multiple traffic accommodation in a subsystem, Table 5 gives the mean and variation statistics of  $I_{(7)}$  in case C. Two situations are considered: In situation “No” only video users (type 3) are accommodated in subsystem 7 and the same number of voice (type 1), fax (type 2), and video (type 3) users are assumed to be accommodated in situation “Yes.” As expected in (14) and (15), the mean is almost the same in both situations and the variance can be reduced in situation “Yes.” However, this reduction is so small and has an insignificant effect on the link capacity. There are so many users even in situation “No.” Hence the additional multiplexing gain due to multiple traffic accommodation is relatively small compared with the gain due to a large number of users in a multiple cell environment.

## 6. Conclusions

In an overlaid multiband CDMA system, a variety of traffic types can be accommodated flexibly. In this paper the reverse link capacity of an SIR-based power-controlled overlaid multiband CDMA system was evaluated in single and multiple cell environments. We applied the recursive calculation method [11], [12] of the mean and variance of other cell interference power developed for an SIR-based TPC system in a multiple cell environment. Spreading bandwidths of 5/10/20 MHz were considered in a multiple class CBR traffic environment. The effect of the spreading pulse shape filter on the mutual interference among subsystems was also considered in the capacity evaluation. By newly introducing a weighted-aggregated data rate as the link capacity, we compared four different combinations of subsystems in terms of maximum link capacity. It was

found that not capacity degradation but a slight capacity gain can be obtained by overlaying subsystems with different spreading bandwidths. The capacity gain is due to the existence of different interference suppression factors, which also necessitates a special CAC scheme to maximize the link capacity and the CAC scheme differs case by case. The capacity of a multiple cell system is reduced by approximately 40% as indicated in [11], [12]. The effect of multiple traffic accommodation in a subsystem was found to be insignificant on link capacity because additional multiplexing gain due to multiple traffic types is relatively small compared with the gain due to a large number of users in a multiple cell environment.

In a multipath environment, the required  $E_b/I_o$  of a user may differ for a different spreading bandwidth because many resolvable paths exist in a wider spreading bandwidth [1]. The voice activity factor may also need to be considered in capacity estimation. If the above problems are to be considered, the analysis may be complicated and tedious, but obtaining the capacity is straightforward. Especially, the effect of the voice activity factor can be estimated from the results in [11], [12]. In this paper, perfect power control was assumed. The capacity degradation due to imperfect power control and the effect of multipath fading are left for future study.

## References

- [1] F. Adachi, A. Sawahashi, and H. Suda, "Wideband DS-CDMA for next-generation mobile communications systems," *IEEE Commun. Mag.*, pp.56–69, Sept. 1998.
- [2] L.B. Milstein, D.L. Schilling, R.L. Pickholtz, V. Erceg, M. Kullback, E.G. Kanterakis, D.S. Fishman, W.H. Biederman, and D.C. Salerno, "On the feasibility of a CDMA overlay for personal communications networks," *IEEE J. Sel. Areas Commun.*, vol.10, pp.655–668, May 1992.
- [3] A. Baier, U.C. Fiebig, W. Granzow, W. Koch, P. Teder, and J. Thielecke, "Design study for a CDMA-based third-generation mobile radio system," *IEEE J. Sel. Areas Commun.*, vol.12, pp.733–743, May 1994.
- [4] K.S. Gilhousen, I.M. Jacobs, R. Padovani, A.J. Viterbi, L.A. Weaver, Jr., and C.E. Wheatley III, "On the capacity of a cellular CDMA system," *IEEE Trans. Veh. Technol.*, vol.40, pp.303–312, May 1991.
- [5] S. Ariyavisitakul, "Signal and interference statistics of a CDMA system with feedback power control," *IEEE Trans. Commun.*, vol.41, pp.1626–1634, Nov. 1993.
- [6] S. Seo, T. Dohi, and F. Adachi, "SIR-based transmit power control of reverse link for coherent DS-CDMA mobile radio," *IEICE Trans. Commun.*, vol.E81-B, no.7, pp.1508–1516, July 1998.
- [7] S. Ariyavisitakul, "Signal and interference statistics of a CDMA system with feedback power control—Part II," *IEEE Trans. Commun.*, vol.42, pp.579–605, Feb./March/April 1994.
- [8] S.J. Lee, H.W. Lee, and D.K. Sung, "Capacities of single-code and multi-code DS-CDMA systems accommodating multimedia services," *IEEE Trans. Veh. Technol.*, vol.48, pp.376–384, March 1999.
- [9] S.J. Lee and D.K. Sung, "Capacity evaluation for DS-CDMA systems with multi-class On/Off traffic," *IEEE Commun. Lett.*, pp.153–155, June 1998.
- [10] D.K. Kim and D.K. Sung, "Power allocation and capacity of an MC-CDMA system supporting heterogeneous CBR and ON-OFF traffic," *Proc. MoMuC*, pp.201–204, Seoul, Korea, 1997.
- [11] D.K. Kim and D.K. Sung, "Capacity estimation for an SIR-based power-controlled CDMA system supporting ON-OFF traffic," *IEEE Trans. Veh. Technol.*, to be published.
- [12] D.K. Kim and D.K. Sung, "Capacity estimation for a multi-code CDMA system with SIR-based power control," *IEEE Trans. Veh. Technol.*, to be published.
- [13] D.G. Jeong, I.G. Kim, and D. Kim, "Capacity analysis of spectrally overlaid multiband CDMA mobile networks," *IEEE Trans. Veh. Technol.*, vol.47, pp.798–807, Aug. 1998.
- [14] F. Adachi, "Theoretical analysis of DS-CDMA reverse link capacity with SIR-based transmit power control," *IEICE Trans. Fundamentals*, vol.E79-A, no.12, pp.2028–2034, Dec. 1996.
- [15] Y.W. Kim, "Radio resource management in multiple-chip-rate DS/CDMA systems supporting multimedia services," Ph.D. dissertation, KAIST, Feb. 1999.
- [16] Y.W. Kim, D.K. Kim, J.H. Kim, S.M. Shin, and D.K. Sung, "Radio resource management in multiple-chip-rate DS/CDMA systems supporting multi-class services," submitted to the *IEEE Trans. Veh. Technol.*
- [17] A. Shitbutani, H. Suda, and F. Adachi, "Multi-stage interleaver for turbo codes in DS-CDMA mobile radio," *Proc. APCC/ICCS*, pp.391–395, Singapore, Nov. 23–27, 1998.
- [18] E. Geraniotis and B. Ghaffari, "Performance of binary and quaternary direct-sequence spread-spectrum multiple-access systems with random signature sequences," *IEEE Trans. Commun.*, vol.39, pp.713–724, May 1991.
- [19] J.G. Proakis, *Digital communications*, McGraw-Hill, 3rd ed., 1995.
- [20] T.S. Rappaport, *Wireless communications: Principles and practice*, Prentice-Hall, 1996.
- [21] F. Adachi and D.K. Kim, "Interference suppression factor in DS-CDMA systems," *Electronics Letters*, vol.35, pp.2176–2177, Dec. 1999.
- [22] Y. Asano, Y. Daido, and J.M. Holtzman, "Performance evaluation for band-limited DS-CDMA communication system," *Proc. VTC*, pp.464–468, Secaucus, USA, 1993.



**Duk Kyung Kim** received the B.S. degree in electrical engineering from Yonsei University, Seoul, Korea, in 1992, and the M.S. and Ph.D. degrees from the Korea Advanced Institute of Science and Technology (KAIST), in 1994 and 1999, respectively. Currently, he is working at the Wireless Laboratories, NTT Mobile Communications Networks, Inc., Japan as a postdoctoral researcher. He was interested in Asynchronous Transfer Mode (ATM) network and ATM-based Personal Communication Service (PCS) network. His research interests now include soft handoff modeling, handoff management, power control, and multimedia provision in CDMA systems, and medium access control for next generation wireless systems (E-mail: kdk@ieee.org).



**Fumiyuki Adachi** received his B.S. and Dr. Eng. degrees in electrical engineering from Tohoku University, Sendai, Japan, in 1973 and 1984, respectively. In 1973, he joined the Electrical Communications Laboratories of Nippon Telegraph & Telephone Corporation (now, NTT) and conducted various research related to digital cellular mobile communications. From July 1992 to December 1999, he was with NTT Mobile

Communications Network, Inc., where he led a research group on wideband/broadband CDMA wireless access for IMT-2000 and beyond. Since January 2000, he has been at Tohoku University, Sendai, Japan, where he is a Professor in the Department of Electrical Communications at Graduate School of Engineering. His research interests are in CDMA and TDMA wireless access techniques, CDMA spreading code design, Rake receiver, transmit/receive antenna diversity, adaptive antenna array, bandwidth-efficient digital modulation, and channel coding, with particular application to broadband wireless communications systems. During the academic year of 1984/85, Dr. Adachi was a United Kingdom SERC Visiting Research Fellow in the Department of Electrical Engineering and Electronics at Liverpool University. From April 1997 to March 2000, he was a visiting professor at Nara Institute of Science and Technology, Japan. He has written chapters of three books: Y. Okumura and M. Shinji, eds., "Fundamentals of mobile communications" published in Japanese by IEICE, 1986; M. Shinji, ed., "Mobile communications" published in Japanese by Maruzen Publishing Co., 1989; and M. Kuwabara, ed., "Digital mobile communications" published in Japanese by Kagaku Shinbun-sha, 1992. He was a co-recipient of the IEICE Transactions best paper of the year award 1996 and again 1998. He is a senior member of the IEEE. He was a co-recipient of the IEEE Vehicular Technology Transactions best paper of the year award 1980 and again 1990 and was also a recipient of Avant Garde Award in 2000.